

Suprathermal rotation of PAHs in the ISM[★]

II. Observational evidence for the rotational broadening of $\lambda 5797$ DIB in reflection nebulae – implication for the carrier size

P. Le Coupanec¹, D. Rouan¹, C. Moutou², and A. Léger³

¹ Observatoire de Paris-Meudon, Département Spatial, CNRS F-92195 Meudon Cedex, France

² Observatoire de Haute-Provence, CNRS, F-04870 Saint-Michel l'Observatoire, France

³ Institut d'Astrophysique Spatiale, CNRS, bat 121, F-91405 Orsay, France

Received 28 July 1998 / Accepted 12 May 1999

Abstract. In a previous paper, we described a model which can explain the $\lambda 5797$ diffuse interstellar band (DIB) profile as seen in absorption in the diffuse interstellar medium and in emission in the Red Rectangle (RR), as a rotational envelope of electronic transitions where the molecular carrier is a free PAH of size ≈ 40 atoms. One of the *strongest predictions* is the behaviour of the rotational temperature of PAH in the case of regions rich in UV such as Reflection Nebulae: it must be suprathermal with respect to the gas temperature but clamped to ≈ 100 K for any PAH size. The width of the DIB, in such regions, can then be broader than in the classical ISM ($T_{\text{rot}} \approx 30$ K) if the values of the molecular transition are favorable. In order to test this prediction, we have obtained high resolution spectra of 27 reddened early type stars, mostly in reflection nebulae, in order to compare their $\lambda 5797$ DIB width to those of stars in classical diffuse interstellar medium. These spectra were made for several DIBs such as $\lambda 5797$, $\lambda 6379$ and $\lambda 6613$, with a spectral resolving power of about 60 000. The analysis of the results agrees with our prediction since the width of the $\lambda 5797$ DIB is broader in a majority of areas with strong UV radiation. Moreover, the broadening is not observed on DIBs $\lambda 6379$ and $\lambda 6613$, indicating that the molecular parameters of the electronic transitions at the origin of the different DIBs are pretty variable from one DIB to another and confirming that the measured broadening on $\lambda 5797$ is not due to an instrumental bias. The statistical measurement of the $\lambda 5797$ width in this medium permits the derivation of new constraints on *the size* of the carrier of this DIB, a molecule that should have 30 to 45 carbon atoms if, as we propose, it is indeed a PAH.

Key words: line: profiles – molecular processes – ISM: molecules – ISM: reflection nebulae

Send offprint requests to: P. Le Coupanec
(patricia.lecoupanec@obspm.fr)

[★] Based on observations made at Observatoire de Haute Provence (CNRS), France

1. Introduction

The question of the origin of the DIBs remains essentially unsolved. At present, the species which are responsible for the bands are still unknown, except a recent plausible identification of C60^+ as carrier of two new diffuse bands, at 9577 and 9632 Å (Foing & Ehrenfreund 1994, 1997). Consequently, major spectroscopic information on the composition and the chemistry of the interstellar medium is still unutilized. However, major results have been obtained by Scarrott et al. (1992): DIBs were seen in emission at least in one object (RR), the widths and position of several of these bands depend upon the distance to the star and are nicely explained by a rotational envelope of electronic transitions in a free molecule. In fact most of the broadening is due to a difference in the rotational constant B between the lower level and the excited level. One shows (Rouan et al. 1997, hereafter RLL) that the width of the DIB is:

$$\Delta(h\nu) = kT_{\text{rot}}\Delta B/B \quad (1)$$

For reasonable values of $\Delta B/B$, a high rotational temperature is deduced ($T_{\text{rot}} > 450$ K) in the RR. We have proposed a model of suprathermal rotation (RLL) that explains both this high temperature and the behaviour with radial distance, assuming that the DIB carrier is a free PAH molecule. Those molecules, originally proposed by Léger & Puget (1984) and Van der Zwet & Allamandola (1985), are good candidates because polycyclic aromatic hydrocarbons are known to be stable gas-phase molecules, able to resist the hard UV field of the interstellar medium, and they might exist in sufficient amounts to affect the reddening curve (Donn 1968). This physical modeling of the rotation of a PAH takes into account several processes of exchange of angular momentum with the ISM. It requires, in particular, a rocket effect, which is the systematic ejection of hydrogen molecules – the analogue of the modified Davies-Greenstein mechanism proposed by Purcell (1975) for the interstellar grains – in order to reproduce the suprathermal rotational temperature observed in the Red Rectangle. Another result of the model is that it agrees with the width of the $\lambda 5797$ DIB observed in the diffuse ISM which is about ≈ 0.75 Å. In addition,

this model allows us to make predictions for the DIB's width in regions exposed to a high UV flux such as reflection nebulae (RN). After the absorption of a UV photon, a PAH cools down by emission of IR photons and gives the well-known UIR bands (Léger & Puget 1984). In conditions of high UV flux and when the matter density is not too high, otherwise the collisions will dominate, the emission of IR photons is the most important process of exchange of angular momentum: it then rules the rotation mechanism and one shows that the rotational temperature is then independent on the incident flux and clamped to 100–120 K whatever the carrier's size is. In such conditions, we predict that DIB's widths in reflection nebulae are significantly larger, typically by 0.3 to 0.4 Å, than those in the ISM where a rotational temperature of 30 K is expected (thermal equilibrium). In RLL we discussed the fact that such a broadening was suggested in spectra presented by Josafatsson & Snow (1987) who especially examined stars in reflection nebulae. However the spectral resolution of those data was not sufficient to conclude firmly. High resolution spectroscopy of several reddened stars has been performed to test the predictions of the model, as well as to constrain the physical properties of the $\lambda 5797$ DIB carrier. Spectra of the narrow DIBs at $\lambda 5797$, $\lambda 6379$ and $\lambda 6613$ with a spectral resolving power of 60 000 have been taken at OHP in 1997. We needed a spectral resolution of at least 0.1 Å to detect an expected broadening effect of 0.3 to 0.4 Å, i.e. a bandwidth larger by 50% of that observed in the ISM.

2. The instrument and observations

The aim was to observe reddened stars (a) which emit a large fraction of their energy in the UV, but still without ionizing significantly the gas and (b) with interstellar matter on the line of sight close to the star, to be sure that molecules there, are subject to strong UV radiation from it ($E_{UV} \approx 50 \text{ eV cm}^{-3}$). Reflection nebulae illuminated by A7-B1 stars are the typical candidates we were looking at. The presence of a reflection nebula is an indication that a fraction of the matter is irradiated by the UV flux but it does not guarantee that this irradiated matter is on the line-of-sight of the target star. In particular, if the illuminated matter is in the background of the star, no broadening will be detected. For instance, this is probably the case of the four Pleiades stars 17, 20, 23 and 25 Tau that we selected because they were in the list of objects observed by Josafatsson & Snow (1987). In order to have statistically enough stars to bring an effect to the fore, we needed a sample of blue stars as large as possible. It consists in 27 stars which were selected in order to fulfil a number of constraints: sufficient reddening, high brightness ($m_V < 7$) and spectral type earlier than A0. Some relevant parameters of the chosen program stars are listed in Table 1. These stars were selected from the sample of stars already observed by Josafatsson & Snow (1987) and from the Van Den Bergh catalogue (1966), they are mostly in reflection nebulae associated to early type stars. A reference star, HD30614, seen through standard diffuse interstellar medium was also observed, for comparison.

Table 1. Program star data: the first list is stars where diffuse bands were detected with a sufficient signal to noise ratio ($S/B > 100$), the second one is stars with a too low signal to noise ratio ($S/B < 100$) and the last one is the reference star)

STAR	S.P.T.	V	E(B-V)
HD2905	B1I	4.16	0.33
HD13267	B5I	6.35	0.41
HD20041	A0I	5.8	0.73
HD23180	B1III	3.82	0.26
HD23478	B3IV	6.67	0.25
HD24398	B1I	2.93	0.31
HD21291	B9I	4.23	0.42
HD21389	A0I	4.54	0.54
HD34078	O9.5V	5.94	0.52
HD43836	B9II	6.95	0.48
HD53367	B0IV	6.94	0.74
HD147010	B9II/III	7.40	0.23
HD183143	B7I	6.84	1.28
HD190603	B1.5I	5.62	0.72
HD199478	B8I	5.67	0.48
HD200775	B2V	7.42	0.57
HD205139	B1II	5.53	0.32
HD209975	O9I	5.11	0.31
HD213087	B0.5I	5.52	0.57
HD216200	B3IV	5.93	0.24
HD217675	B6III	3.62	0.05
HD23302 (17 Tau)	B6III	3.7	0.02
HD23408 (20 Tau)	B8III	3.87	0.05
HD23480 (23 Tau)	B6IV	4.18	0.08
HD23630 (25 Tau)	B7III	2.9	0.03
HD37903	B1.5V	7.83	0.36
HD30614	O9.5I	4.29	0.26

The observations were carried out during two observing periods in March 1997 and in September 1997 with the spectrograph AURELIE at the Coude focus of the 1.52 m telescope at the Observatoire de Haute Provence, France (Gillet et al. 1994). The detector is a 2048 photodiodes linear Reticon array with $750 \times 13 \mu\text{m}^2$ pixels, which is read by a Thomson TH7832 CCD system of two alternately reading CCDs. Only one grating was used, with $1.2 \cdot 10^4 \text{ lines cm}^{-1}$ giving a resolution in the spectral ranges where we observed of $R = 60\,000$. This grating is used in combination with a filter OG515 in order to avoid second order image overlap. Each resolution element is fully sampled by three pixels of the CCD, i.e. 0.03 \AA/px . The resolution element is 0.096 \AA which is necessary to measure a broadening effect of 0.3–0.4 Å. Four different wavelength ranges were observed in order to study the possible width variations of several DIBs. One was centered on 5870 Å to measure the Na D lines for measuring the velocity profile induced by clouds on the various lines of sight and the three others were centered on DIBs 5797, 6379 and 6613 Å. Telluric lines, originating in the Earth's atmosphere, were detected in the spectrum of the fast rotating unreddened B3V star HD120315. To isolate DIBs from stellar lines, we have observed 11 non-reddened stars with spectral types similar to those of the target objects.

3. Data processing

3.1. Instrumental effects

The observed spectra are corrected for detector offset and pixel to pixel sensitivity variations (flat fielding), by means of offset exposures and using a Tungsten calibration lamp respectively. The dark current was found to be negligible. The telluric and stellar lines are identified from spectra of the observed calibration stars. Each spectrum is divided by the spectrum of a reference star with a close stellar type in order to have a flat continuum around the analyzed diffuse band. Then, the continuum is normalized to unity and interpolated at the line position with a parabolic fit, this operation inducing only a small error. The wavelength scale was calibrated with exposures on a Thorium-Argon emission lamp. Data reduction was made at the Observatoire de Paris-Meudon using the IDL software.

3.2. Line width extraction

This width comparison with the reference star is not obvious: we must take into account the different processes which can affect the width of the observed DIB. There could be possibly numerous clouds in the line of sight and important turbulences inside each cloud. The Na D lines were used to quantify the contribution of the intervening clouds in the DIB broadening. This effect can be deconvolved from the width of the diffuse band observed in order to obtain a representative width of the intrinsic DIB profile in the UV irradiated environment. Each NaD velocity profile was assumed to be gaussian in order to fit the line, including possible saturation effect. The comparison method comprises two steps:

- (1) the diffuse band $\lambda 5797$ of the reference star HD30614 is deconvolved by its own fitted velocity profile deduced from NaD lines to obtain the intrinsic feature's profile for this star
- (2) this reference DIB of the diffuse medium is convolved with the fitted velocity profile of the target star observed

The procedure is valid as long as the DIB feature is optically thin, which is always the case. At this stage, it is as if both diffuse bands, measured on the reddened target star and the reference, were seen through the "same" line of sight, i.e. with the same cloud velocity profile. It is then justified to compare the two $\lambda 5797$ bands, with depth normalized to 1, as it is their physical width corresponding to the rotational envelope which interests us. The widths of the diffuse band and the reference are measured in Å at three different levels: 50 %, 30 % and 60 % of the maximum in order to have a mean width independent on the possibly blended bands and on the asymmetrical profile of the DIB.

4. Results

The RLL model indicates that there should be a suprathermal rotation of PAHs in regions where the UV flux is high, but the model makes another important prediction: this physical broadening must be *quite constant*. Indeed, in such regions

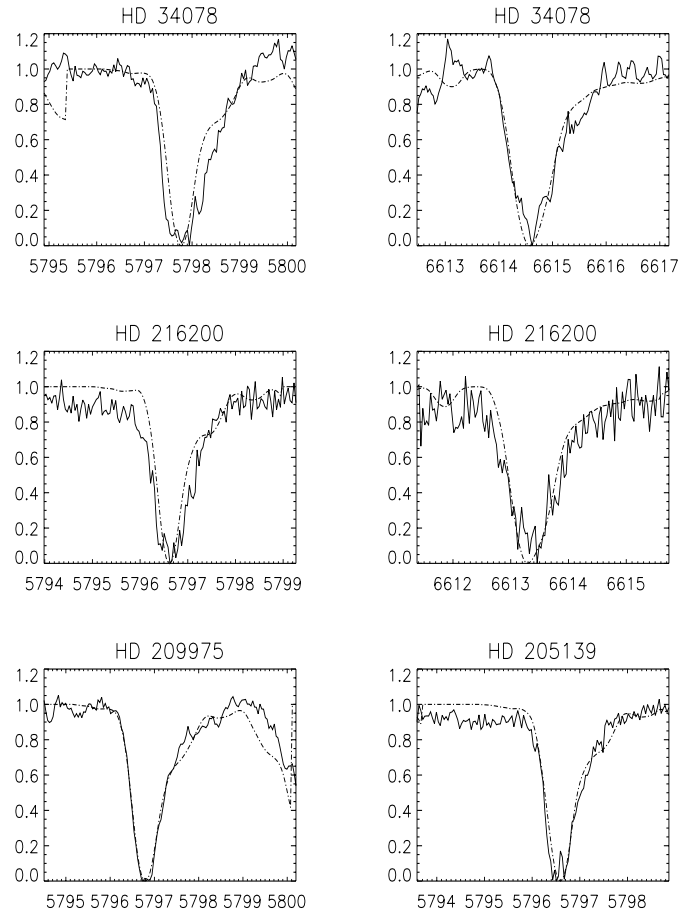


Fig. 1. Spectra of $\lambda 5797$ and $\lambda 6613$ DIB of target stars superimposed on the reference star (dot-dash lines) which would be observed towards a similar line of sight: on the top, HD34078 has a clear broadening for the $\lambda 5797$ and not for the $\lambda 6613$ – in the middle, HD216200 with the same results – at the bottom, HD209975 and HD205139 which have not a $\lambda 5797$ broadened.

where the UV flux is strong (typically of 50 eV cm^{-3}), the rotational temperature is locked around 100 K whatever the carrier's size is. So, for a given ro-vibrational transition, the physical width of the diffuse band must be almost the same as soon as $E_{\text{UV}} > 50 \text{ eV cm}^{-3}$. In a first step we have used the differential method of Sect. 3.2, i.e. as free as possible from instrumental bias and effects of intervening clouds, in order to reveal some systematic broadening in RN, and secondly, we have tried to derive the best estimate of the intrinsic bandwidth which carries the actual information on rotation.

4.1. The $\lambda 5797$ broadening

On a statistical sample of 27 stars observed, 21 of them have diffuse bands detected with a sufficient signal-to-noise ratio ($S/N > 100$). Table 2 gives for each star observed, the interstellar extinction evaluated from $E(B-V)$ and taken as $3.1 E(B-V)$, the difference of width measured at 50% of the DIB depth and the average one between the levels at 30% and 60% between the target star and the interstellar medium star, corrected as depicted

Table 2. Measured width difference between the target star and the reference star HD30614 seen through the same Doppler profile at half maximum of the DIB depth. Column (4) is the average broadening between the two levels at 30% and 60%. The last column lists the width of the “intrinsic” $\lambda 5797$ DIB measured.

STAR	$A_v = 3.1E(B-V)$	$\Delta\lambda_{FWHM}$ (\AA)	$\Delta\lambda_{<30,60\%>}$ (\AA)	$\Delta\lambda_{int}$ (\AA)
HD2905	1.02	0.22	0.15	0.70
HD13267	1.27	0.16	0.1	0.67
HD20041	2.26	0.02	0.04	0.50
HD23180	0.80	0.25	0.25	0.79
HD23478	0.77	0.22	0.23	0.65
HD24398	0.96	0.21	0.20	0.62
HD21291	1.3	0.28	0.20	0.78
HD21389	1.74	0.22	0.18	0.76
HD34078	1.5	0.36	0.34	0.90
HD43836	1.4	0.18	0.15	0.76
HD53367	2.3	0.05	-0.04	0.50
HD147010	0.8	0.28	0.20	0.78
HD183143	3.96	0.19	0.18	0.68
HD190603	2.23	0.20	0.16	0.75
HD199478	1.48	0.02	0.01	0.50
HD200775	1.77	0.06	0.03	/
HD205139	1.12	0.10	0.08	0.53
HD209975	1.08	0.02	0.	0.50
HD213087	1.76	0.13	0.15	0.60
HD216200	0.74	0.29	0.22	0.76
HD217675	0.15	0.01	0.02	0.45

above. As an illustration, six resulting spectra for the $\lambda 5797$ and $\lambda 6613$ are plotted in Fig. 1 where the solid line is the target DIB and the dash-dotted line is the reference star. The two on the top are stars which show clearly a broadening for the $\lambda 5797$ and not for the other two DIBs observed, while the two on the bottom do not have a broadened $\lambda 5797$ and fit the reference profile quite well.

Table 2 shows that 14 stars out of 21, that is to say 66% of the sample, exhibit a diffuse band $\lambda 5797$ significantly larger than the same band arising from the interstellar diffuse medium where density and radiative conditions are different. The other 34% with no broadened DIB may be explained by stars with no matter close to them or with a line of sight configuration which does not fill our criteria. The broadening varies from 0.1 to 0.3 \AA between the reference star HD30614 and the different lines of sight. This is somewhat lower than what was roughly derived by RLL from data of Josafatsson & Snow (1987). However, the uncertainty on the width estimate we derived, from their published spectra, was probably too large for an accurate validation of our prediction. The result of our dedicated observations is that we have *actually observed that the $\lambda 5797$ diffuse band shows a broadening* towards a large fraction of stars associated with strong UV irradiated regions. The most obvious case is HD34078 which is illuminating a reflection nebula where $\lambda 5797$ is broader by about 0.34 \AA than the reference star seen through its line of sight. Among the sample of 14 stars, 7 cases (or 50%) have a broadening of more than 0.2 \AA compared to the

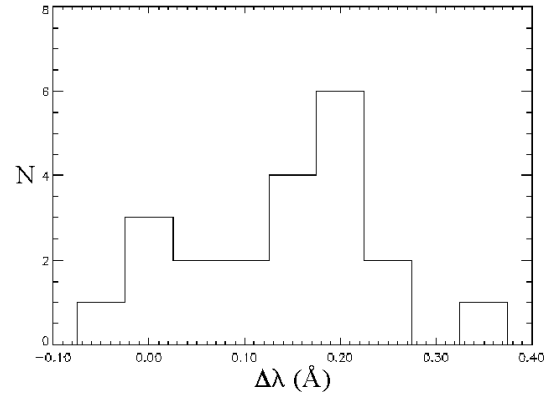


Fig. 2. Histogram showing the distribution of the average broadening compared to the reference star for all observed targets for the $\lambda 5797$ DIB.

reference star and 7 stars (or 50%) have one in the range 0.1 to 0.2 \AA . When the measured broadening was lower than 0.1 \AA , we considered that there was no effect. These results are summarized on the histogram of Fig. 2. We have checked that no bias is introduced by some peculiarity of the reference HD30614 since we obtained the same results using HD209975 another classical standard in DIB studies.

For the other two DIBs at $\lambda 6379$ and $\lambda 6613$, such broadening of the band *has not been detected* even in the targets where the $\lambda 5797$ DIB is unambiguously broader. This lack of broadening for two other DIBs is not in contradiction with our prediction for $\lambda 5797$, because ΔB can be much lower for the corresponding transitions, the carrier being the same or not. On the contrary, this behaviour proves that our processing is valid and does not introduce significant artefacts.

4.2. The intrinsic width

A second part of the processing on the spectra was to use the information on the line of sight carried by the Na D components to derive the “intrinsic” $\lambda 5797$ DIB profile for each star. Now, each $\lambda 5797$ diffuse band was deconvolved by the velocity profile deduced from Na D lines for all target stars observed. Then, the average width ($\frac{\Delta\lambda(30\%)+\Delta\lambda(60\%)}{2}$) measured on the “intrinsic” DIB is considered as the width *proper* to the rotational envelope only. Those “intrinsic” widths are listed in the last column of Table 2 and the corresponding histogram is on Fig. 3. It shows that the sample is split as expected into two families:

- one has intrinsic widths centered around 0.50 \AA which correspond to the group of stars where there is no broadening compared to the diffuse interstellar medium
- the other one, with widths > 0.70 \AA , is correlated with the sample in which an actual broadening has been observed.

The rather smooth distribution could reflect the fact that the lines-of-sight toward reflection nebula stars contain matter close to the star as well as general interstellar matter in varying ratios even if the matter close to the star consistently produces a $\lambda 5797$ DIB with $FWHM=0.8$. So, an average width of about 0.75 \AA for

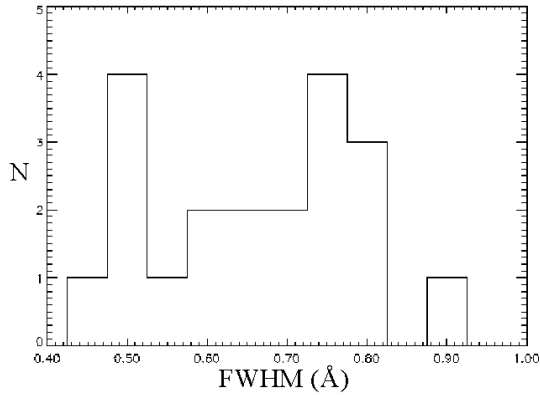


Fig. 3. Histogram showing the distribution of the FWHM measured for the intrinsic width of the $\lambda 5797$ DIB of all target stars.

the $\lambda 5797$ DIB in regions exposed to UV flux can be estimated. It allows us to derive information on the size of the carrier which will be discussed in the next section.

4.3. Environmental variations of DIB profile in individual stars

The spectra were obtained with a good signal-to-noise ratio (> 100) and with a high resolution ($\approx 0.03 \text{ \AA}/\text{pixel}$). Furthermore each band was observed several times, these independent exposures allowing to test whether substructures in the band are real. An important sample of $\lambda 5797$ diffuse bands was obtained: it shows on the one hand that this band possesses multiple substructures as previously indicated by Ehrenfreund & Foing (1996, 1995), Krelowski & Schmidt (1997), and Sarre et al. (1995) and on the other hand that this structured profile differs from one star to the other. This finding certainly deserves to be studied more deeply because it may be possible to find a relationship between the radiation density and variations in the DIB substructures.

The reflection nebulae associated with the Pleiades stars, for example, were observed and exhibit a very weak $\lambda 5797$ DIB. Maybe, it is because the carrier is destroyed in this region. Another interesting sample of stars are those which belong to the Perseus OB2 association (HD23180, HD24398 and HD23478): these stars are obscured by an extended molecular cloud, as already shown on the CO map observed by Ungerechts & Thaddeus (1987), and we note that all three present an obvious broadening.

In the same way, the case of HD216200 is interesting; it is not in the VDB catalogue but shows an important broadening. In fact, this star seems to be a binary system of a B3e primary and a F9IV secondary in which the latter loses mass towards the primary and creates a disk around it (Hill et al. 1997). The questions are now: are the diffuse bands observed towards this target formed in the disk? and are the carriers able to survive in such an environment?

Furthermore, the two well-known reflection nebulae NGC2023 and NGC7023 were observed and show weak $\lambda 5797$ DIBs. It is known for a long time that the diffuse bands there, are systematically weak compared to normal diffuse interstellar

medium (Snow et al. 1977, 1995; Walker et al. 1980; Josafatsson & Snow 1987). An interpretation could be that in these regions, the UV flux from the star is too strong and destroys the DIB's carriers. For both stars, we cannot detect any broadening effect because of the low signal-to-noise ratio.

5. Discussion

5.1. Local extinction and broadening

We observed that several strongly reddened stars illuminating reflection nebulae exhibit in their spectrum a broader $\lambda 5797$ DIB compared to the diffuse medium. This result is a strong indication, but not, however, a definite proof that the measured broadening is due to actually irradiated matter on the line of sight. A strong support for our prediction would be to show that, when detected, the broadening of $\lambda 5797$ is associated with a sufficient amount of irradiated gas close to the star and *on the line of sight*. We looked for such a correlation using different methods.

- A model of the interstellar extinction taking into account the distance of the star and its galactic latitude was used to deduce for each star a mean extinction $A_{v,m}$ which can be expressed as:

$$A_{v,m} \approx [Z_0 \cdot \frac{(1 - \exp(-\frac{D|\sin b|}{Z_0}))}{|\sin b|}] * 1.9$$

where Z_0 is the height scale of absorption above the galactic plane ($Z_0 = 140 \text{ pc}$), D is the distance of the star, b is its galactic latitude and the mean interstellar extinction used there, was of 1.9 mag/kpc . Then this mean computed extinction was compared to the actual extinction observed towards the star and we tried to find a correlation between the excess of extinction and the excess of broadening. However, it could not be established because many of the stars have a reddening lower than the mean extinction derived from the model. It probably shows that any model of the interstellar extinction at large scale is not valid at the level of individual stars because of the heterogeneous distribution of interstellar dust.

- We tried to trace the absorbing matter close to the star by its IR emission. The idea was to derive a local extinction from the ratio between the far infrared luminosity of the surrounding dust and the bolometric luminosity of the dereddened star. But it was not possible to have for a sufficient number of cases, a good enough evaluation of the infrared flux which was tentatively derived from the IRAS data. For instance, only 28% of the stars in our sample were listed by Gaustad & Van Buren (1993) as extended objects having an excess of emission at $60 \mu\text{m}$, which indicates the presence of interstellar dust at the location of the star.
- Another method was to compare the B-V histogram of the actual star distribution in a narrow cone around the target star (PMM USNO_A1.0 catalogue, Monet 1996) and a model of stellar population of the Galaxy (Robin & Crz 1986). The correlation between the observation (PMM) and the model

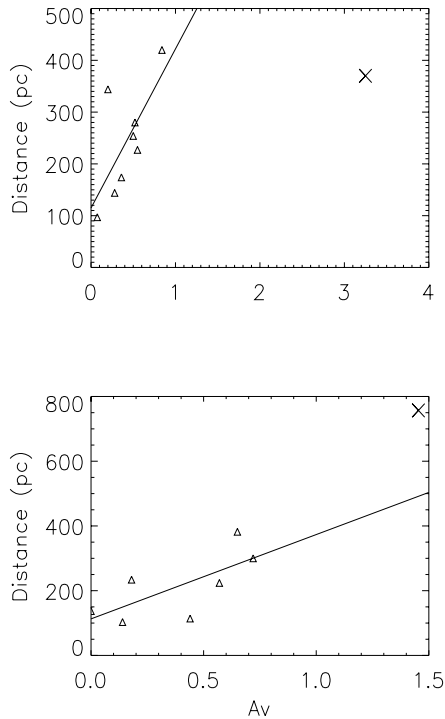


Fig. 4. Linear regression between distance and extinction A_v in the line of sight towards target stars from the Hipparcos catalogue, crosses indicate the target star: (*up*) for HD183143, there is an obvious excess of extinction; (*down*) for HD 21389, it shows no evidence of an excess for this star, despite the broadening of the $\lambda 5797$ DIB in front of it.

(Besançon) was made by fitting the parameter of mean interstellar extinction in mag/kpc which is adjustable in the model of Besançon. This method again did not work because stars in our sample are in general not very far (about 500 pc on average) and the foreground stars do not represent more than 1% of all stars detected in the PMM catalogue for each line of sight. Thus, it was impossible to conclude about the mean extinction in front of each target star in the corresponding direction of the Galaxy.

- d) The purpose of the last modelling was to estimate the extinction along the line of sight by using data of the Hipparcos catalogue. All the stars inside 1 degree of field from target were recorded. The Hipparcos catalogue provided their distance and we plotted the extinction A_v of each star versus its distance. Then, using a linear regression of the distribution, our aim was to conclude that our targets showed an excess of extinction. The problem was that the parallax given by Hipparcos are affected by large error bars when the distance overtakes 500 pc, and so the linear regression is too uncertain. In most cases it was not possible to reach a conclusion. Two examples (Fig. 4) are given above to illustrate a successful case and another which fails.

To sum up, a direct correlation between the $\lambda 5797$ band broadening and the presence of absorbing matter close to the star could not be established systematically. Only in a few cases, for instance HD21389, is a clear indication of nearby matter both

from IRAS and Hipparcos data found, but this is not statistically significant: it is certain that the sample of stars must be greater to reveal a real trend.

5.2. Constraints on the $\lambda 5797$ DIB carrier size

In the Red Rectangle, it was only possible to derive the product $T_{\text{rot}} \cdot \Delta B/B$ from the width of $\lambda 5797$ (see Eq. 1). As shown in RLL, in reflection nebulae, the rotational temperature is almost independent on the carrier size and imposes the value of $\Delta B/B$ by removing the degeneracy in the product $kT_{\text{rot}} \cdot \Delta B/B$. As shown by our observations the $\lambda 5797$ DIB intrinsic width in those regions is about 0.75 \AA . This value injected in the rotational model gives new constraints on the size of the carriers if they are PAH molecules. We have to take into account a term which was neglected in the case of the RR which is the P,Q and R branches separation, in addition to the broadening induced by change in the rotational constant. The width of the band is then approximated by the following expression (RLL):

$$\Delta(h\nu) \approx 2.5kT_{\text{rot}} \Delta B/B + 4\sqrt{BkT_{\text{rot}}} \quad (2)$$

The width of the band, expressed in wave number (cm^{-1}), is written as:

$$\Delta\sigma \approx 1.74T_{\text{rot}}\Delta B/B + 5.81N_c^{-1}\sqrt{T_{\text{rot}}} \quad (\text{cm}^{-1}) \quad (3)$$

with: $B = 5 \cdot 10^{-4} (N_c/78)^{-2}$.

From RLL (Fig. 8), we can derive an empirical relationship, valid for the ISM, between the rotational temperature and the number of carbon atoms N_c , which reads:

$$T_{\text{rot}}^{\text{ISM}} \approx A (N_c/78)^{1.7}$$

with A ranging from 152 K to 254 K, depending on the environmental conditions. The system of the two equations (3), one for each case of the ISM and RN, has two unknown quantities which are the rotational temperature in the ISM ($T_{\text{rot}}^{\text{ISM}}$) and $\Delta B/B$ corresponding to the $\lambda 5797$ transition. Using the intrinsic width of the band for the ISM and for reflection nebulae of 0.50 \AA and 0.75 \AA (see Sect. 4.2) respectively and considering that the rotational temperature in reflection nebulae is 100 K (RLL), we can then resolve the system and derive $\Delta B/B$ and N_c for the $\lambda 5797$ carrier. The solution for this nominal set of parameters is:

$$\Delta B/B = 0.33\%, \quad T_{\text{rot}}^{\text{ISM}} = 52 \text{ K} \quad \text{and} \quad N_c = 35.$$

Large uncertainties may come from the approximated law $T_{\text{rot}}^{\text{ISM}}$ versus N_c and from the approximation of the P,Q and R branches contribution in Eq. (2). We looked for a range of solutions allowing the parameters to vary within reasonable limits. This then lead to a range of $\Delta B/B$ between 0.13% ($T_{\text{rot}}^{\text{ISM}}=47 \text{ K}$) and 0.72% ($T_{\text{rot}}^{\text{ISM}}=59 \text{ K}$) and to a typical number of carbon atoms for the $\lambda 5797$ DIB carrier between 30 and 45. This evaluation is consistent with other range proposition made by different authors on the basis of the IR emission (Puget & Léger 1989) or using the rotational contour modelling of the peak separation in the $\lambda 5797$ DIB substructures (Ehrenfreund & Foing 1996).

6. Conclusion

High resolution spectra of reddened stars illuminating reflection nebulae were obtained. Using a method where, as far as possible, observational bias is minimized – this is checked on other DIBs –, we show that the $\lambda 5797$ DIB appear broader than in the diffuse ISM towards a significant fraction of the sample of target stars. We claim that this result does agree with a prediction we made previously (RLL), assuming that the carrier of the DIB is a free PAH molecule in the interstellar medium. One important prediction of this model is the expected behaviour of the rotational temperature towards stars embedded in reflection nebulae, where the irradiation is stronger. A constant temperature of ≈ 100 K was predicted in any situation and for any size of the carrier. Because its width increases linearly with rotational temperature the $\lambda 5797$ DIB is a good thermometer, sensitive enough to check the prediction. We interpret the lack of broadening on the rest of the sample as a lack of UV-irradiated matter on the line of sight, a plausible situation, but unfortunately any attempt to correlate the broadening with another indication (IR excess, extinction excess) of matter close to the star than the presence of a reflection nebula has been unsuccessful. Because the predicted rotational temperature in reflection nebulae is constrained to a very small range around 100 K, we are able to derive $\Delta B/B$ from the bandwidth, since $\Delta\lambda \propto T_{\text{rot}} \cdot \Delta B/B$. We derive a measured intrinsic width of the $\lambda 5797$ DIB in reflection nebulae of about $\Delta\lambda = 0.75$ Å; this leads to a value of $\Delta B/B$ ranging between 0.13% and 0.72% i.e., smaller than estimated by RLL. Using now this value of $\Delta B/B$ in the case of the diffuse ISM, we can constrain the rotational temperature from the observed DIB bandwidth, which, in turns, leads to an estimate of the size of the carrier from the model. This size between 30 and 45 carbons is consistent with the most likely size of the carrier molecules (if PAH) as currently proposed in the DIB study.

Acknowledgements. We thank the referee, A.N. Witt, for his fruitful comments which helped to improve the paper. Our thanks are extended to the staff of OHP for their welcome and assistance during the observations, and to C. and G. Robichez for their careful reading of the paper which lead to some useful suggestions. P. Le Coupanec acknowledges MESR (Ministre de l'Enseignement Supérieur et de la Recherche, France) for a doctoral fellowship.

References

- Donn B., 1968, ApJ 152, L129
 Ehrenfreund P., Foing B.H., 1995, CCP7/PCMI Newsletter 22, 18
 Ehrenfreund P., Foing B.H., 1996, A&A 307, L25
 Foing B.H., Ehrenfreund P., 1994, Nat 369, 296
 Foing B.H., Ehrenfreund P., 1997, A&A 319, L59
 Gaustad J.E., Van Buren D., 1993, PASP 105, 1127
 Gillet D., Burnage R., Kohler D., et al., 1994, A&AS 108, 181
 Hill G., Harmanec P., Pavlovski K., et al., 1997, A&A 324, 965
 Josafatsson K., Snow T.P., 1987, ApJ 319, 436
 Krelowski J., Schmidt M., 1997, ApJ 477, 209
 Léger A., Puget J. L., 1984, A&A 137, L5
 Monet D., 1996, A&AS 188, 5404
 Puget J.L., Léger A., 1989, ARA&A 27, 161
 Purcell E.M., 1975, In: Field G.B., Cameron A.G.W. (eds.) The Dusty Universe
 Robin A., Crz M., 1986, A&A 157, 71
 Rouan D., Léger A., Le Coupanec P., 1997, A&A 324, 661
 Sarre P.J., Miles J.R., Kerr T.H., et al., 1995, MNRAS 277, L41
 Scarrott S.M., Watkin S., Miles J.R., Sarre P.J., 1992, MNRAS 255, 11P
 Snow T.P., York D.G., Welty D.E., 1977, AJ 82, 113
 Snow T.P., Bakes E.L.O., Buss R.H. Jr., Seab C.G., 1995, A&A 296, L37
 Ungerechts H., Thaddeus P., 1987, ApJS 63, 645
 Van den Bergh S., 1966, AJ 71, 990
 Van der Zwet G. P., Allamandola L. J., 1985, A&A 146, 76
 Walker G.A.H., Yang S., Fahlman G.G., Witt A.N., 1980, PASP 92, 411